JOURNAL OF THEORETICAL AND APPLIED MECHANICS
3, **39**, 2001

THREE-DIMENSIONAL ELASTIC AND ELASTO-PLASTIC FRICTIONAL CONTACT ANALYSIS OF TURBOMACHINERY BLADE ATTACHMENTS

Grzegorz Zboiński
Wiesław Ostachowicz

Institute of Fluid Flow Machinery, Polish Academy of Sciences
e-mail: zboi@imppan.imp.pg.gda.pl

The paper presents a summary of the research on three-dimensional contact analysis of turbomachinery blade attachments in the elastic and elasto-plastic range. In that context the paper deals with theoretical, methodological and phenomenological description of the problem. The paper focuses on the applied variational formulation of contact problems of elasticity and elasto-plasticity and the corresponding finite element methods, utilizes contact mechanics algorithms as well as describes displacement, stress, contact and slip states within real turbomachinery blade attachments. Non-linear character of contact mechanics procedures and influence of these nonlinearities on stress and deformation within the attachments are treated with special care.

Key words: finite elements, contact mechanics, elasticity, elasto-plasticity

1. Introduction

We will start this paper with presentation of three different aspects dealt with in the topic. Firstly we will express some general remarks concerning complexity of of the analysis under consideration. Then development and state of the art will be presented. We will end up with research issues and authors' contribution to the subject.

1.1. General remarks

Contact analysis of turbomachinery blade attachments constitutes a very good example of how recent advances of contemporary mechanical and com-

puter science can influence our approach to the solution of complex technological problems. The analysis of turbomachinery blade attachments is not a new task for turbomachinery engineeres. The numerical tools, however, that are at their disposal are still in progress. That is why the quality of finite element (FE) analysis of turbomachinery blade attachments is still being improved. Note that the main difficulties in modeling and analysis of such objects arise from their complexity, i.e. highly complicated geometrical form as well as strong non-linearity of the related phenomena caused by plasticity and friction (physical non-linearity) as well as the changing contact zone (geometrical non-linearity) of two parts of the attachment, i.e. blade root and grooved disc sector. It is clear that analysis of such problems can be a challange from both the engineering and scientific points of view.

Defining precisely our requirements for proper modeling and sufficiently accurate FE analysis of blade attachments, we should mention the following factors affecting the numerical solution:

- three-dimensional character of the attachment geometry and loading as well as of the resulting strain and stress states,
- elastic or elasto-plastic properties of the bodies in contact (blade root and disc sector),
- geometrically non-linear character of contact (generally unknown contact zone) due to unilateral contact constraints,
- friction occuring between contacting bodies,
- three-dimensional character of cyclo-symetric and support constraints on the outer boundaries of the disc sector of the attachment.

1.2. State of the art

There were (or should we say, there are) four main steps in the development of application of the finite element methods to the analysis of blade attachments. The first step started in early 1970s with plane elastic models loaded by concentrated forces and subject to simplified boundary and stable frictionless contact conditions (Gontarovskiĭ et al., 1978; Nigin, 1976). At the same time the plane elastic models were enriched by inclusion of friction (Chan and Tuba, 1971). The next step which began in early 1980s accounted for elasto-plastic plane models, firstly without (Gontarowskiĭ and Kirkach, 1982) and later with friction (Bloch and Orobinskiĭ, 1983). The third stage started in late 80s and was caused by advances in computer technology (increase of internal memories of the available machines) and resulted in transition

to three-dimensional attachment models. Again, elastic models without friction for very simple geometry (Alderson et al., 1967) and for complicated ones (Ikeda et al., 1989; Teper and Moore, 1989; Robertson and Walton, 1990) were analysed first, and then friction was included (Zboiński, 1993d). At the present stage, three-dimensional elasto-plastic models without friction are often employed (Rao et al., 2000; Meguid et al., 2000). Inclusion of friction to such models has become a fact (Zboiński and Ostachowicz, 1997a,b).

Two importatant comments concerning the past and contemporary FE calculations are necessary. Firstly, there has been a great deal of work done in this area by various manufacturers, usually by means of commercial computer codes. Much of this work is of considerably high quality. However, manufacturers have generally not decided to present the results of their work in the accessible literature. And secondly, the nowadays available very efficient and general commercial tools for technological FE calculations may not fulfill the specific needs of the user when non-standard, non-linear models of materials, friction and contact are of interest. For example, comparing friction modeling capabilities of NASTRAN (1995), ABAQUS (1995) and ADINA (1999) with the capabilities of the code utilized in this paper (Zboiński and Ostachowicz, 1997b), one can notice that only the latter one accounts for changing friction coefficient.

1.3. Contribution of the authors

Contribution of the authors to the subjects concerning the FE contact analysis of turbomachinery elements can be described as follows. The general incremental local and variational formulations for elastic contact problems which can be applied to derivation of the corresponding finite element methods was presented by Zboiński (1993c, 1995a). The specific variational principle and the basis of the corresponding finite element method applied to contact problems of turbomachinery blade attachments can be found in the paper by the same author (1993e). The algorithms and computer programs corresponding to this method are described by Zboiński in (1993a) and (1993b), respectively. Various aspects of stress, strain and contact analysis of real turbomachinery blade attachments in the elastic range are included in the following papers: Zboiński (1992, 1993d, 1995b). The methods, algorithms and computer programs were then extended by Zboiński and Ostachowicz (1997a,b) to elasto-plastic contact problems. This paper completes the presentation of the research on application of elasto-plastic contact analysis to turbomachinery elements. The main objective here is to show some spectacular results of elasto-plastic stress and contact states within real turbomachinery blade

attachments. Some qualitative comparisons of these results with the case of attachments operating in the elastic range will also be given.

2. The method and algorithm of the analysis

2.1. Local and variational formulation

We consider the incremental contact problem of two elasto-plastic or elastic bodies in common non-inertial reference frame with global Cartesian coordinates $\boldsymbol{X}$. The motion in the reference system is assumed to be caused by small deformations. The local matrix formulation of the problem consists of the equation of motion, constitutive relations of elasto-plasticity (or elasticity), and kinematic relations $(\boldsymbol{X} \in \overset{a}{V})$

$$\begin{aligned} &\Delta\boldsymbol{\sigma}^{j}_{,j} + \Delta\boldsymbol{f} - \overset{a}{\rho}\,[\Delta\boldsymbol{a} + (\boldsymbol{\Omega}^{\top}\boldsymbol{\Omega} + \mathbf{E})\Delta\boldsymbol{q} + (\Delta\boldsymbol{\Omega}^{\top}\Delta\boldsymbol{\Omega} + \Delta\mathbf{E})\boldsymbol{X}] = \mathbf{0} \\ &\Delta\boldsymbol{\sigma} = \overset{a}{\mathbf{D}}\,(\Delta\boldsymbol{\varepsilon} - \overset{a}{\alpha}\,\Delta T\boldsymbol{g}) \\ &\Delta\boldsymbol{\varepsilon} = \boldsymbol{\Gamma}\Delta\boldsymbol{q} \end{aligned} \tag{2.1}$$

which hold in volumes $\overset{a}{V}$ of each body $a = 1, 2$. The matrix of elasto-plastic properties (see Zboiński and Ostachowicz, 1997a) and the six-component stress and strain increment vectors are denoted $\overset{a}{\mathbf{D}}$, $\Delta\boldsymbol{\sigma}$, $\Delta\boldsymbol{\varepsilon}$, respectively. The term $\Delta\boldsymbol{\sigma}^{j}$ is a global vector component $(j = 1, 2, 3)$ of the stress increment vector, while $\boldsymbol{\Gamma}$ stands for the matrix derivative operator transforming the displacement increment vector $\Delta\boldsymbol{q}$ into the strain vector. Increments $\Delta\boldsymbol{f}$ and $\Delta\boldsymbol{a}$ are due to the body force and translation acceleration, respectively. The known skew-symmetric matrices of angular velocity and acceleration increments are denoted $\Delta\boldsymbol{\Omega}$ and $\Delta\mathbf{E}$ while their total values from the previous incremental step are denoted with $\boldsymbol{\Omega}$ and $\mathbf{E}$. The initial incremental strains due to the scalar stationary incremental temperature field ΔT are defined by the coefficient of thermal expansion $\overset{a}{\alpha}$ and six-component Cartesian metric vector $\boldsymbol{g}$.

The stress boundary conditions holding on the part $\overset{a}{P}$ of the body surface can be written in the following matrix form

$$\Delta\boldsymbol{\sigma}\boldsymbol{\nu} = \Delta\boldsymbol{p} \qquad \boldsymbol{X} \in \overset{a}{P} \tag{2.2}$$

where the quantities $\Delta\boldsymbol{\sigma}$, $\Delta\boldsymbol{p}$ and $\boldsymbol{\nu}$ are the stress increment matrix, surface traction increment vector and the unit exterior normal vector, respectively.

Additionally, on the part $\overset{a}{Q}$ of the body surface the incremental kinematic boundary conditions and stress relations hold

$$\Delta \boldsymbol{q} = \Delta \boldsymbol{d} \qquad \Delta \boldsymbol{\sigma\nu} = \Delta \boldsymbol{r} \qquad \boldsymbol{X} \in \overset{a}{Q} \tag{2.3}$$

Terms $\Delta \boldsymbol{d}$ and $\Delta \boldsymbol{r}$ in the above relations stand for the known values of displacement increments and the unknown values of surface stress reaction vector increments, respectively.

The incremental contact mechanics equations valid on the common contact surface K of the two bodies contain vectors $\boldsymbol{n}$ and $\mathbf{t}$: unit exterior vector normal to K and the matrix of vectors of two unit tangents of the lower numbered body $(a = 1)$. The one-component vector of gap $\boldsymbol{h}_n$ is expressed in terms of the initial gap vector $\boldsymbol{h}_{0n}$ and normal displacement increments $\Delta \overline{\boldsymbol{q}}_n$ and total values $\overline{\boldsymbol{q}}_n$. Note that both the latter vectors are defined as differences of the proper quantities of the first and second body, for example: $\Delta \overline{\boldsymbol{q}}_n = \Delta \overset{1}{\boldsymbol{q}}_n - \Delta \overset{2}{\boldsymbol{q}}_n$. Four terms: $\Delta \boldsymbol{r}_n$, $\boldsymbol{r}_n$, $\Delta \boldsymbol{r}_t$, $\boldsymbol{r}_t$ denote incremental and total (known from the previous incremental step) values of normal and tangential components of the surface reaction vectors. The two-component vector of slip increment $\Delta \boldsymbol{s}_t$ is expressed in terms of tangential displacement increments $\Delta \overline{\boldsymbol{q}}_t$ defined as a difference of the displacements of two bodies in contact: $\Delta \overline{\boldsymbol{q}}_t = \Delta \overset{1}{\boldsymbol{q}}_t - \Delta \overset{2}{\boldsymbol{q}}_t$. The function Δg represents increment of the tangential traction bound, while $\mathbf{C}$ is a general surface constitutive matrix of either Coulomb or elasto-Coulombian slip rule. Using such notions the mentioned equations of contact mechanics can be written as $(\boldsymbol{X} \in K)$

$$\begin{aligned}
&\boldsymbol{n}^{\top} \Delta \boldsymbol{\sigma\nu} = \Delta \boldsymbol{r}_n && \mathbf{t}^{\top} \Delta \boldsymbol{\sigma\nu} = \Delta \boldsymbol{r}_t \\
&\Delta \overline{\boldsymbol{q}}_n + \overline{\boldsymbol{q}}_n + \boldsymbol{h}_{0n} = \boldsymbol{h}_n && \boldsymbol{h}_n \cdot \Delta \boldsymbol{r}_n = 0 \\
&\boldsymbol{h}_n \cdot \boldsymbol{r}_n = 0 && \Delta r_n \leqslant 0 \\
&r_n \leqslant 0 && \Delta \boldsymbol{s}_t = \Delta \overline{\boldsymbol{q}}_t \\
&\sqrt{\Delta \boldsymbol{s}_t \cdot \Delta \boldsymbol{s}_t}(\sqrt{\Delta \boldsymbol{r}_t \cdot \Delta \boldsymbol{r}_t} + \Delta g) = 0 && \sqrt{\Delta \boldsymbol{s}_t \cdot \Delta \boldsymbol{s}_t}(\sqrt{\boldsymbol{r}_t \cdot \boldsymbol{r}_t} + \mu r_n) = 0 \\
&\sqrt{\Delta \boldsymbol{r}_t \cdot \Delta \boldsymbol{r}_t} + \Delta g + b \leqslant 0 && b = \sqrt{\boldsymbol{r}_t \cdot \boldsymbol{r}_t} + \mu r_n \leqslant 0 \\
&\sqrt{\Delta \boldsymbol{s}_t \cdot \Delta \boldsymbol{s}_t} \geqslant 0 && \Delta \boldsymbol{s}_t = \mathbf{C} \Delta \boldsymbol{r}_t
\end{aligned} \tag{2.4}$$

One shoud notice that the above set of relations correspond to the case of Coulombian slip rule for which one can distinguish between adhesion, slip and gap states. For the case of the model based on elasto-Coulombian slips, for which adhesion state does not exist four last but one equations have to be

rejected. The specific form of the surface constitutive laws for both mentioned cases can be found in (Zboiński and Ostachowicz, 1997a).

A variational formulation corresponding with the above local realtions (2.1)-(2.4) takes the incremental version of the Hamilton principle as a basis. The formulation presented here assumes that two last equations of (2.1), first equality (2.3) and all except the first, second, sixth, thirteenth and fifteenth relations (2.4) hold. Thus the proper variational inequality (see Zboiński and Ostachowicz, 1997a) can be written as

$$\begin{aligned}
&\sum_{a=1}^{2}\Big\{\int\limits_{\overset{a}{V}}\{\delta(\Delta\boldsymbol{\varepsilon}^{\top})\overset{a}{\mathbf{D}}(\Delta\boldsymbol{\varepsilon}-\overset{a}{\alpha}\Delta T\boldsymbol{g})-\delta(\Delta\boldsymbol{q}^{\top})\Delta\boldsymbol{f}-\\
&-\delta(\Delta\boldsymbol{q}^{\top})\overset{a}{\rho}[\Delta\boldsymbol{a}+(\boldsymbol{\Omega}^{\top}\boldsymbol{\Omega}+\mathbf{E})\Delta\boldsymbol{q}+(\Delta\boldsymbol{\Omega}^{\top}\Delta\boldsymbol{\Omega}+\Delta\mathbf{E})\boldsymbol{X}]\}\,d\overset{a}{V}-\\
&-\int\limits_{\overset{a}{P}}\delta(\Delta\boldsymbol{q}^{\top})\Delta\boldsymbol{p}\,d\overset{a}{P}-\int\limits_{\overset{a}{Q}}\delta(\Delta\boldsymbol{q}^{\top})\Delta\boldsymbol{r}\,d\overset{a}{Q}\Big\}-\\
&-\int\limits_{K}[\delta(\sqrt{\Delta\boldsymbol{s}_t\cdot\Delta\boldsymbol{s}_t})\Delta g+\delta(\Delta\overline{\boldsymbol{q}}_n^{\top}+\overline{\boldsymbol{q}}^{\top}+\boldsymbol{h}_{0n}^{\top}-\boldsymbol{h}_n^{\top})\Delta\boldsymbol{r}_n+\\
&+\delta(\Delta\overline{\boldsymbol{q}}_t^{\top}-\Delta\boldsymbol{s}_t^{\top})\Delta\boldsymbol{r}_t]\,dK\leqslant 0
\end{aligned}\tag{2.5}$$

The inequality form of the above principle is caused by unilateral normal contact conditions and existence of tangential traction bound in the case of Coulombian slips. For the case of elasto-Coulombian slips, one should replace in (2.5) the term $\delta(\sqrt{\Delta\boldsymbol{s}_t\cdot\Delta\boldsymbol{s}_t})\Delta g$ accounting for either adhesion or the slip states with $\delta(\Delta\boldsymbol{s}_t^{\top})\Delta\boldsymbol{r}_t$ which corresponds to the slip state only. After such a change, the inequality form of the principle is still preserved due to unilateral normal contact constraints.

In order to derive one general method of solution of the Coulombian and elasto-Coulombian problems under consideration we can propose the introduction of the proper reduced contact problem at each incremental step, as one of the possibilities. The suggested method is based on the assumption that the potential contact area which is divided either into adhesion, slip or gap (Coulombian model) or slip and gap (elasto-Coulombian one) parts, does not change within the incremental or iterative step of the solution procedure. Note that the three parts of the potential contact area are denoted by letters A, S and G, respectively. The mentioned divisions need employing the proper criteria based on inequalities from the set (2.4). In particular, we use the sixth and eighth relations to choose between the gap and contact states, while the twelvth and fourteenth relations are used to distinguish between the adhesion

and slip states. Additionally, in our formulation we have to take into account that: the work of tangential tractions is done only on the part S, for parts A and S the relation $h_n = 0$ holds, whereas on A we have $\Delta \boldsymbol{s}_t = \boldsymbol{0}$. Moreover, we assume that the tangential traction bound increment and slip increments are known in each iterative step of the solution process. We denote the known values of these quantities by $\Delta g \equiv \mu \Delta p_n$ and $\Delta \boldsymbol{s}_t \equiv \Delta \boldsymbol{z}_t$. Use of the above notions, expression of the slip increments $\delta(\Delta \boldsymbol{s}_t)$ through the tangential displacement increments $\delta(\Delta \overline{\boldsymbol{q}}_t)$, and change of surface degrees of freedom (DOFs) $\Delta \overline{\boldsymbol{q}}_n$, $\Delta \overline{\boldsymbol{q}}_t$ into global DOFs $\Delta \overline{\boldsymbol{q}}$ in $\boldsymbol{X}$-directions by means of relations: $\Delta \overline{\boldsymbol{q}}_n = \boldsymbol{n} \Delta \overline{\boldsymbol{q}}$, $\Delta \overline{\boldsymbol{q}}_t = \mathbf{t} \Delta \overline{\boldsymbol{q}}$ allows to write the proper stationarity principle corresponding to Coulomb slips in the following form

$$
\begin{aligned}
&\sum_{a=1}^{2} \Big\{ \int_{\overset{a}{V}} \{ \delta(\Delta \boldsymbol{\varepsilon}^{\top}) \overset{a}{\mathbf{D}} (\Delta \boldsymbol{\varepsilon} - \overset{a}{\alpha}\, \Delta T \boldsymbol{g}) - \delta(\Delta \boldsymbol{q}^{\top}) \Delta \boldsymbol{f} - \\
&- \delta(\Delta \boldsymbol{q}^{\top})\, \overset{a}{\rho}\, [\Delta \boldsymbol{a} + (\boldsymbol{\Omega}^{\top} \boldsymbol{\Omega} + \mathbf{E}) \Delta \boldsymbol{q} + (\Delta \boldsymbol{\Omega}^{\top} \Delta \boldsymbol{\Omega} + \Delta \mathbf{E}) \boldsymbol{X}] \}\, d\, \overset{a}{V} - \\
&- \int_{\overset{a}{P}} \delta(\Delta \boldsymbol{q}^{\top}) \Delta \boldsymbol{p}\, d\, \overset{a}{P} - \int_{\overset{a}{Q}} \delta(\Delta \boldsymbol{q}^{\top}) \Delta \boldsymbol{r}\, d\, \overset{a}{Q} - \\
&- (-1)^{a+1} \Big[\int_{S} \delta(\Delta \boldsymbol{q}^{\top}) \frac{\mathbf{t} \Delta \boldsymbol{z}_t \mu \Delta p_n}{\sqrt{\Delta \boldsymbol{z}_t \Delta \boldsymbol{z}_t}}\, dS + \int_{S} \delta(\Delta \boldsymbol{q}^{\top}) \boldsymbol{n} \Delta r_n\, dS + \\
&+ \int_{A} \delta(\Delta \boldsymbol{q}^{\top}) \Delta \boldsymbol{r}\, dA \Big] \Big\} = 0
\end{aligned}
\tag{2.6}
$$

while for the elasto-Coulombian case we can write

$$
\begin{aligned}
&\sum_{a=1}^{2} \Big\{ \int_{\overset{a}{V}} \{ \delta(\Delta \boldsymbol{\varepsilon}^{\top}) \overset{a}{\mathbf{D}} (\Delta \boldsymbol{\varepsilon} - \overset{a}{\alpha}\, \Delta T \boldsymbol{g}) - \delta(\Delta \boldsymbol{q}^{\top}) \Delta \boldsymbol{f} - \\
&- \delta(\Delta \boldsymbol{q}^{\top})\, \overset{a}{\rho}\, [\Delta \boldsymbol{a} + (\boldsymbol{\Omega}^{\top} \boldsymbol{\Omega} + \mathbf{E}) \Delta \boldsymbol{q} + (\Delta \boldsymbol{\Omega}^{\top} \Delta \boldsymbol{\Omega} + \Delta \mathbf{E}) \boldsymbol{X}] \}\, d\, \overset{a}{V} \\
&- \int_{\overset{a}{P}} \delta(\Delta \boldsymbol{q}^{\top}) \Delta \boldsymbol{p}\, d\, \overset{a}{P} - \int_{\overset{a}{Q}} \delta(\Delta \boldsymbol{q}^{\top}) \Delta \boldsymbol{r}\, d\, \overset{a}{Q} - \\
&- (-1)^{a+1} \Big[\int_{S} \delta(\Delta \boldsymbol{q}^{\top}) \mathbf{t} \Delta \boldsymbol{t}_t\, dS + \int_{S} \delta(\Delta \boldsymbol{q}^{\top}) \boldsymbol{n} \Delta r_n\, dS \Big] \Big\} - \\
&- \int_{S} \delta(\Delta \overline{\boldsymbol{q}}^{\top}) \mathbf{t} \mathbf{k}_t \mathbf{t}^{\top} \Delta \overline{\boldsymbol{q}}\, dS = 0
\end{aligned}
\tag{2.7}
$$

It is worth noticing that we replaced differences $\Delta\overline{\boldsymbol{q}}$ with increments $\Delta\boldsymbol{q}$ of each of two bodies in contact in (2.5) and (2.6), when it was posssible. Note also that in the last relation, $\mathbf{k}_t$ and $\Delta\boldsymbol{t}_t$ represent the surface constitutive matrix corresponding to slip increments and tangential traction increment vector due to normal traction increment (compare Zboiński and Ostachowicz, 1997a). We should underline that two above relations constitute a starting point for introduction of one general algorithm for two finite element methods of contact problems of elastoplasticity. Elucidation of these methods can be found in the paper cited above.

2.2. Some details of the algorithm

A full algorithm for the FE solution of the problems under consideration consists of generation of the element stiffness matrices and force increments vectors, structure stiffness and force increment formation, solution of the set of nonlinear algebraic equations and frictional contact algorithms. The former two parts of the procedure have the property that they correspond with the standard FE algorithms for non-linear elastoplastic problems, while the latter two include the non-standard, non-linear aspects of the contact analysis. The simplified flow diagram of the algorithm is presented in Fig. 1. Note that two different procedures corresponding to Coulomb (C-model) and elasto-Coulombian (EC-model) models are combined in one general algorithm with the proposed approach. This algorithm is utilized in the computer program PLAST presented in (Zboiński and Ostachowicz, 1997b) which is applied to the research conducted in this paper.

Details of the above algorithm were presented in the previous work by the authors (Zboiński and Ostachowicz, 1997a). Here we restrict ourselves to some original aspects concerning the calculation of friction stiffnesses and forces which both reflect the physical non-linearity of the contact. The first important feature of the proposed approach is introduction of all friction terms on the global level, i.e. through nodal surface stiffness and nodal friction forces of the structure instead of defining them on the element level. We should stress that the global nodal description of friction forces has been succesfully applied to problems with Coulombian models accounting only for non-reversible (Coulombian slips) and neglecting elastic (reversible) slips. On the contrary, introduction of the friction terms to elasto-Coulombian models has been performed on the element level through element vectors of frictional stresses and element surface stiffnesses, so far. The reason for this is dependence of the elastic part of the surface stiffness on discretization of the contact area. Hence, in order to introduce the friction terms on the global nodal level, we have to

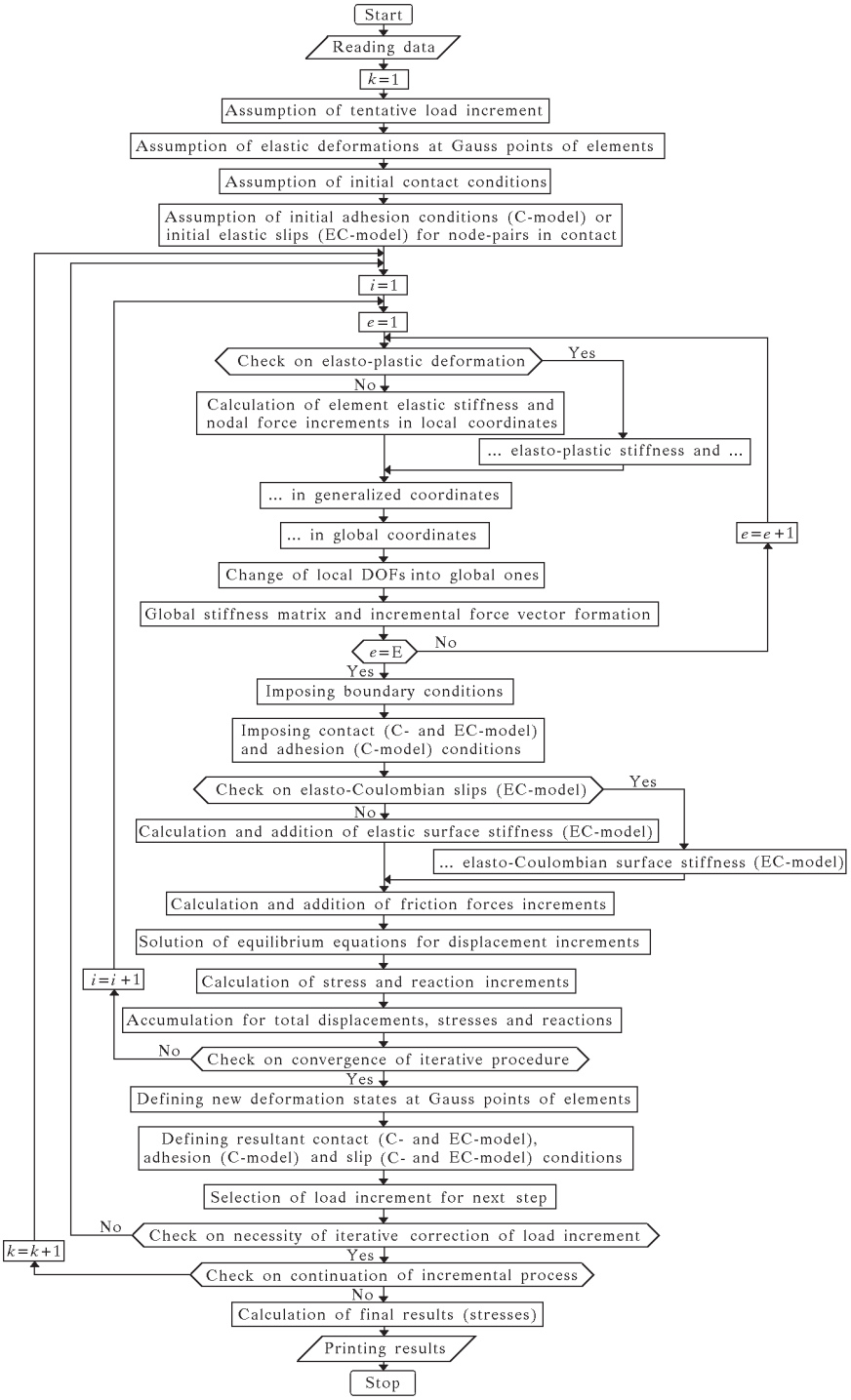

Fig. 1. General algorithm for frictional elastic and elasto-plastic contact analysis

overcome the problem of discretization, or should we say, of assignment of the the contact area to a global (structure) contact node. The proper method is given below.

The second feature of the proposed approach deals with the solution method of the contact problems, which assumes a reduced problem at each incremental and iterative step of the solution process. Such an assumption leads to linearization of the FE element equilibrium equations. In practice it means that the global surface stiffness $\overset{i}{\mathbf{K}}_t$ (included only for the case of elasto-Coulombian friction) defined for any pair of nodes I and J of the first and second body, respectively, as well as the global incremental friction forces $\Delta \overset{i}{\boldsymbol{T}}_t$ at node I, which both depend on the unknown displacement increments, are prescribed at any step i of the solution procedure. The assumed to be known values of the nodal vectors of the normal traction increments $\Delta \overset{i}{P}_n$, total surface tractions $\overset{i}{\boldsymbol{P}} = \operatorname{col}[\overset{i}{\boldsymbol{P}}_t, \overset{i}{P}_n]$ and slip increments $\Delta \overset{i}{\boldsymbol{Z}}_t$ are used for the purpose of friction terms determination and are assumed to be equal to the proper resultant values from the previous step $i-1$, i.e.

$$\begin{aligned} &\Delta \overset{i}{P}_n = \Delta \overset{i-1}{R}_n && \overset{i}{\boldsymbol{P}}_t = \overset{i-1}{\boldsymbol{T}}_t \\ &\overset{i}{P}_n = \overset{i-1}{R}_n && \Delta \overset{i}{\boldsymbol{Z}}_t = \Delta \overset{i-1}{\boldsymbol{S}}_t \end{aligned} \tag{2.8}$$

For the elasto-Coulombian model of friction, contribution of the surface constitutive stiffness of the pair of nodes I and J to the global equilibrium equation is

$$\delta(\Delta \overline{\boldsymbol{q}}_t^{\top}) \overset{i}{\mathbf{K}}_t \Delta \overline{\boldsymbol{q}}_t = \left[\delta(\Delta \overset{1}{\boldsymbol{q}}_t^{\top}), \delta(\Delta \overset{2}{\boldsymbol{q}}_t^{\top})\right] \begin{bmatrix} \overset{i}{\mathbf{K}}_t & -\overset{i}{\mathbf{K}}_t \\ -\overset{i}{\mathbf{K}}_t & \overset{i}{\mathbf{K}}_t \end{bmatrix} \begin{bmatrix} \Delta \overset{1}{\boldsymbol{q}}_t \\ \Delta \overset{2}{\boldsymbol{q}}_t \end{bmatrix} \tag{2.9}$$

where each matrix block $\overset{i}{\mathbf{K}}_t$ is given by

$$\overset{i}{\mathbf{K}}_t = \begin{bmatrix} \overset{i}{K}_{t_{11}} & \overset{i}{K}_{t_{12}} \\ \overset{i}{K}_{t_{21}} & \overset{i}{K}_{t_{22}} \end{bmatrix} \tag{2.10}$$

and terms $\overset{i}{K}_{t_{kl}}$ $(k,l,m=1,2)$ are defined as follows

$$\overset{i}{K}_{t_{kl}} = -kA_I \left(\delta_{kl} - \beta \frac{kA_I}{\overset{i}{P}} \frac{\overset{i}{P}_{t_k} \overset{i}{P}_{t_l}}{\overset{i}{P}_{t_m} \overset{i}{P}_{t_m}} \right) \tag{2.11}$$

with δ_{kl} being the Kronecker symbol, while contribution of the increments of friction forces at node I to the same global equilibrium equations can be defined by

$$\delta(\overset{1}{\Delta \boldsymbol{q}}{}_t^{\top})\Delta \overset{i}{\boldsymbol{T}}_t = \left[\delta(\overset{1}{\Delta} q_{t_1}), \delta(\overset{1}{\Delta} q_{t_2})\right] \begin{bmatrix} \Delta \overset{i}{T}_{t_1} \\ \Delta \overset{i}{T}_{t_2} \end{bmatrix} \tag{2.12}$$

with terms $\Delta \overset{i}{T}_{t_k}$ given by the following formula

$$\Delta \overset{i}{T}_{t_k} = -\beta \frac{kA_I}{\overset{i}{P}} \frac{\overset{i}{P}_{t_k}}{\sqrt{\overset{i}{P}_{t_m} \overset{i}{P}_{t_m}}} \mu \Delta \overset{i}{P}_n \tag{2.13}$$

In the above relations $\beta = 0$ defines the case of elastic slips whereas for $\beta = 1$ the slips are elasto-Coulombian. Constant k characterizes the surface elastic properties while the auxiliary term $\overset{i}{P}$ can be calculated according to

$$\overset{i}{P} = kA_I + \frac{\partial \mu}{\partial \sqrt{\Delta S^c_{t_m} \Delta S^c_{t_m}}} \frac{\Delta \overset{i}{Z}_{t_m} \overset{i}{P}_{t_m}}{\sqrt{\Delta \overset{i}{Z}_{t_m} \Delta \overset{i}{Z}_{t_m}} \sqrt{\overset{i}{P}_{t_m} \overset{i}{P}_{t_m}}} \overset{i}{P}_n \tag{2.14}$$

Note that the term $\partial \mu / \partial \sqrt{\Delta S^c_{t_m} \Delta S^c_{t_m}}$ represents a known relation between the friction coefficient and the Coulombian part of slip. This relation corresponds to elasto-Coulombian slip rule with hardening. The term A_I stands for the contact area assigned for node I or J ($A_I \equiv A_J$) and can be obtained through summation of contact areas a_{e_I} assigned to nodes of the elements e_I meeting at node I

$$A_I = \sum_{e_I=1}^{E_I} a_{e_I} \tag{2.15}$$

where E_I stands for total number of elements forming the contact area under consideration. The elemental part of the contact area can be defined as follows

$$a_{e_I} = \int_{A_e} N_I N_I \, dA_e \tag{2.16}$$

with A_e standing for the element face within contact surface and N_I being the shape function assigned to element node I.

Subsequently, for the Coulombian model of friction we have to introduce only the vector of increments of friction forces updated within each step of the

solution procedure. The components of this vector are

$$\Delta \overset{i}{T}_{t_k} = -\frac{\overset{i}{P}_{t_k}}{\sqrt{\overset{i}{P}_{t_m}\overset{i}{P}_{t_m}}}\mu\Delta \overset{i}{P}_n \tag{2.17}$$

Note that for ideal Coulombian slip rule also another equivalent representation is possible

$$\Delta \overset{i}{T}_{t_k} = -\frac{\Delta \overset{i}{Z}_{t_k}}{\sqrt{\Delta \overset{i}{Z}_{t_m}\ \Delta \overset{i}{Z}_{t_m}}}\mu\Delta \overset{i}{P}_n \tag{2.18}$$

Note that when necessary (change from adhesion to slip), in order to stabilize and thus to speed up the iteration process for the latter case of Coulombian model, one can use the relaxation method which assumes

$$\Delta \overset{i}{T}_{t_k} = (1-\alpha)\Delta \overset{i-1}{T}_{t_k} + \alpha\Delta \overset{i}{T}_{t_k} \tag{2.19}$$

with α standing for the relaxation factor.

3. Elastic and elasto-plastic contact analysis of real blade attachments

3.1. Applied FE models of real attachments

The applied examples of real turbomachinery blade attachments (see e.g. Fig. 2) as utilized in this research are the same as in our previous attempts (Zboiński, 1993d, 1995b; Zboiński and Ostachowicz, 1997b). The corresponding FE models of a single blade airfoil and root as well as a disc sector with a single groove consist of either about 40 thousand DOFs and five thousand isoparametric solid elements or about thertis thousand DOFs and four thousand elements. These two cases correspond to the attachments operating within elastic or elasto-plastic ranges, respectively. In both models the first-order and second-order solid elements as well as mixed-order transition elements (from first- to second-order solid elements) are employed. The second-order elements are applied in the most-stressed regions of the attachment (minimum neck sections of the root and disc as well as contact surfaces of hooks). For other less-stressed parts of the attachment, first-order elements are applied. One layer of the transition elements is utilized in order to join the first-order and

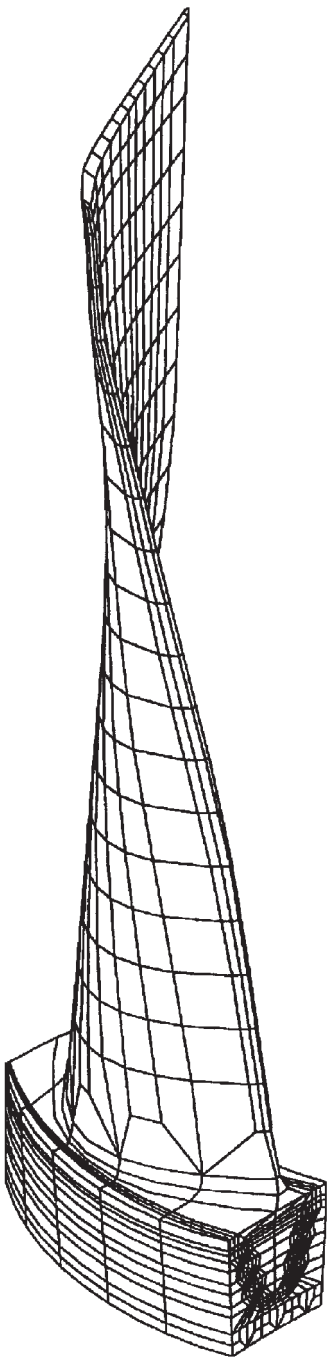

Fig. 2. Exemplary mesh of the blade, root and disc sector of the attachment

second-order regions together. The elements are put into 11 layers parallel to the attachment disc mid-plane. The FE mesh details are those shown in Fig. 3 for the attachment blade root and disc sector.

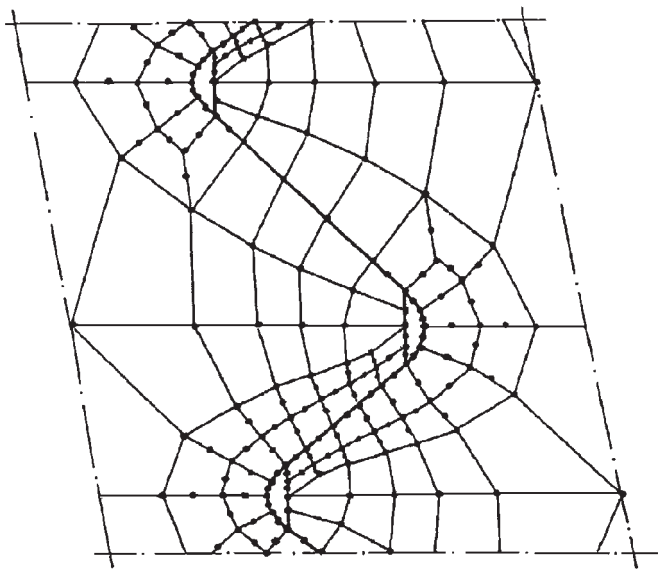

Fig. 3. Mesh details within cross-section of a single contact surface

3.2. Elastic analysis of frictional contact problem

The first example deals with the incremental elastic frictional contact analysis of an axial entry, curved, fir-tree attachment of the blade, with four pairs of root and groove hooks on each side of the attachment. The attachment curvature radius is 0.125 m, a shift of the curvature center from the disc middle plane is 0.025 m. The attachment is loaded by the blade 0.39 m long of the first stage of the low pressure part of the 200 MW steam turbine. The blade rotating at the angular velocity of 3.1415×10^2 1/s (3000 rpm) produces the centrifugal force equal to 109.146 kN acting on the root platform 0.0078 m thick. The outer radius of the disc is 0.519 m, the inner one is 0.250 m, the disc (and attachment) thickness is 0.085 m, while the number of the blade attachments on the disc circumference is 82. Young's modulus of the root and blade material equals $1.94 \times 10^{11}\,\mathrm{N/m^2}$, whereas the modulus of the disc material is $1.88 \times 10^{11}\,\mathrm{N/m^2}$. The material densities and Poisson's ratios are assumed to be equal to the values of $0.78 \times 10^4\,\mathrm{kg/m^3}$ and 0.3, respectively. Four cases

corresponding to geometrically nonlinear contact problem (unknown geometry of contact) are included. The first case deals with the physically linear (frictionless) contact problem, while the rest three cases refer to physically non-linear (frictional) contact problems. The constant and uniform Coulomb friction coefficient μ for the latter three cases equals 0.05, 0.10 and 0.15, respectively.

An example of effective stress distribution within the attachment for the case 1 is shown in Fig. 4. It corresponds to the middle cross-section of the attachment. Effective stress isolines from 1 to 8 correspond to the values changing proportionally from 0.25×10^8 to $2.00 \times 10^8\,\mathrm{N/m^2}$. Note that for the rest three cases stress distribution is qualitatively the same. For all four cases the maximal normal contact stresses within the maximally loaded contact surfaces as a function of friction coefficient are presented below in Table 1. For cases 1 and 4, additionally, the initial and resultant contact statuses of contact nodes within maximally stressed contact surfaces are shown in Table 2. Note that the equivalent initial and resultant statuses corresponding to adhesion, slip and gap are denoted with symbols: A, S and G, respectively, while transition from adhesion to slip, from adhesion to gap and from slip to gap are denoted as: A/S, A/G, S/G, respectively.

Table 1. Maximal normal contact stresses for the elastic cases 1-4

Case	Normal contact stresses $[10^8\,\mathrm{N/m^2}]$					
	Location (lowest left hooks)			Location (highest right hooks)		
	Left edge	Middle	Right edge	Left edge	Middle	Right edge
1	1.931	0.726	0.557	1.380	0.604	0.458
2	1.685	0.577	0.666	1.176	0.493	0.525
3	1.586	0.495	0.707	1.043	0.431	0.564
4	1.532	0.460	0.719	0.974	0.406	0.583

Table 2. Map of initial and resultant contact status for elastic cases 1 and 4

Case	Node location	Initial and resultant status of contact nodes											
		Node layer (lowest left hooks)						Node layer (highest right hooks)					
		1	2	3	4-10	11	12	1	2	3	4-10	11	12
1	Left	S	S	S	S	S	S	S/G	S/G	S/G	S	S	S
	Middle	S	S	S	S	S	S	S	S	S	S	S	S
	Right	S/G	S	S	S	S	S	S	S	S	S	S	S
4	Left	A/S	A/S	A/S	A/S	A/S	A/S	A/G	A/G	A/G	A/S	A/S	A/S
	Middle	A/S	A/S	A/S	A/S	A/S	A/S	A/S	A/S	A/S	A/S	A/S	A/S
	Right	A/G	A/S	A/S	A/S	A/S	A/S	A/S	A/S	A/S	A/S	A/S	A/S

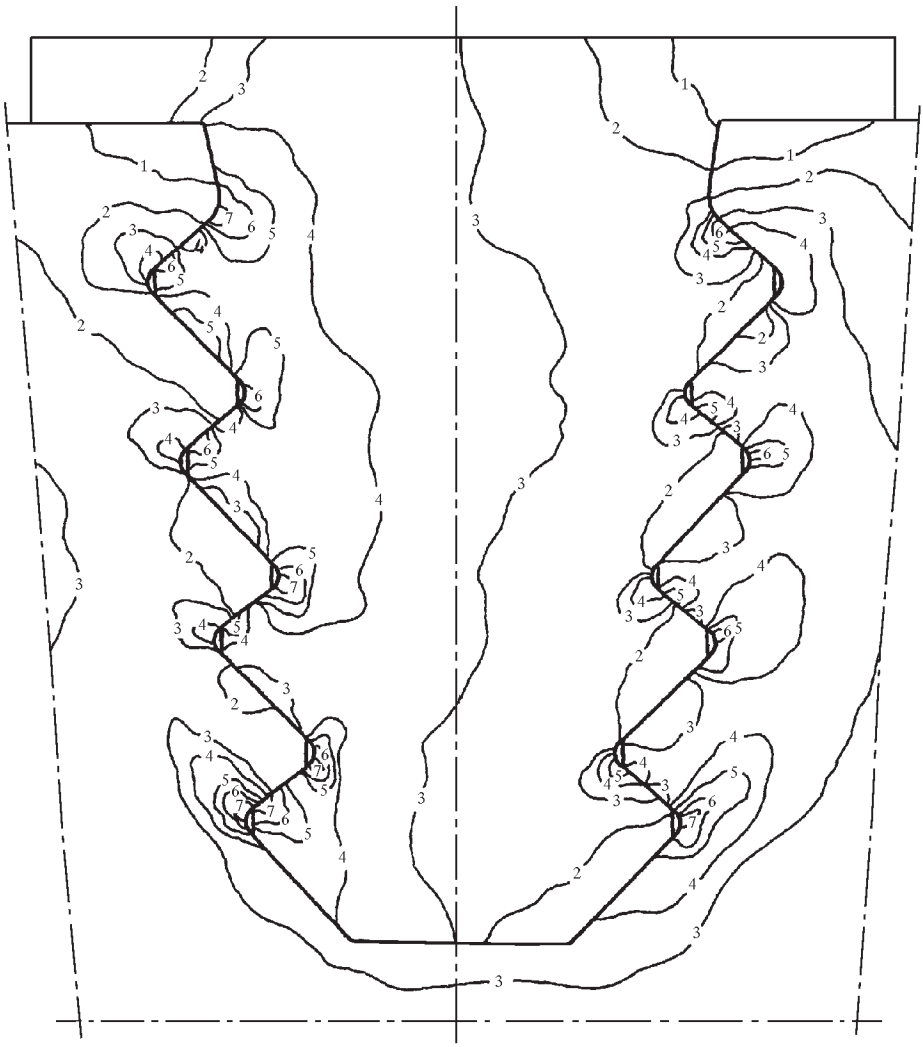

Fig. 4. Elastic effective stress in the cross-section of the attachment

It is worth noting that the stress distribution within the attachment is typical. It means that high values of effective stresses appear at the minimum neck sections or the adjacent contact surfaces of the root and disc, and the maximal values correspond to the first left root and fourth right disc hooks. It is interesting to notice that inclusion of friction ($\mu = 0$ in comparison to $\mu = 0.05$) changes the values of contact stresses much more than further increase of friction coefficient ($\mu = 0.10$ and $\mu = 0.15$). Note also that inclusion of friction diminishes the contact stresses and does not affect the tendency to gap appearance.

3.3. Elasto-plastic analysis of frictional contact problem

The second example deals with the elasto-plastic frictionless contact analysis of an axial entry, curved, fir-tree attachment of the blade, with three pairs of root and groove hooks on each side of the attachment. The attachment curvature radius is 0.185 m, the shift of the curvature center from the disc middle plane is 0.024 m. The attachment is loaded by the blade 0.71 m long of the penultimate stage of the low pressure part of a steam turbine. The blade rotating at the angular velocity of 3.1415×10^2 1/s (3000 rpm) produces the centrifugal force equal to 110.503 kN acting on the root platform 0.0075 m thick. The outer radius of the disc is 0.705 m, the inner one is 0.250 m, the disc (and attachment) thickness is 0.190 m, while the number of the blade attachments on the disc circumference is 53. Young's modulus of the root and blade material equals $1.94 \times 10^{11}\,\mathrm{N/m^2}$, whereas the modulus of the disc material is $1.88 \times 10^{11}\,\mathrm{N/m^2}$. The material densities and Poisson's ratios are assumed to be equal to $0.78 \times 10^4\,\mathrm{kg/m^3}$ and 0.3, respectively. The yield points of the blade root and disc materials are $530 \times 10^6\,\mathrm{N/m^2}$ and $540 \times 10^6\,\mathrm{N/m^2}$, respectively. The common value of the plastic modulus is $0.01 \times 10^{11}\,\mathrm{N/m^2}$. Again four cases are analysed, the first one of which corresponds to geometrically non-linear contact problem with $\mu = 0$, while the next three cases to geometrically and physically nonlinear contact with μ equal to: 0.05, 0.10 and 0.15.

An example of effective stress distribution within the attachment for the case is shown in Fig. 5. It corresponds to the middle cross-section of the attachment. Effective stress isolines from 1 to 5 correspond with values changing proportionally from 1.00×10^8 to $3.00 \times 10^8\,\mathrm{N/m^2}$. The last isoline (denoted with number 6) corresponds to the value of effective stress equal to $5.35 \times 10^8\,\mathrm{N/m^2}$. Hence the regions of elasto-plastic deformation can be easily recognized as those neighboring the last isoline. As before, for all four cases the maximal normal contact stresses within the maximally loaded contact sur-

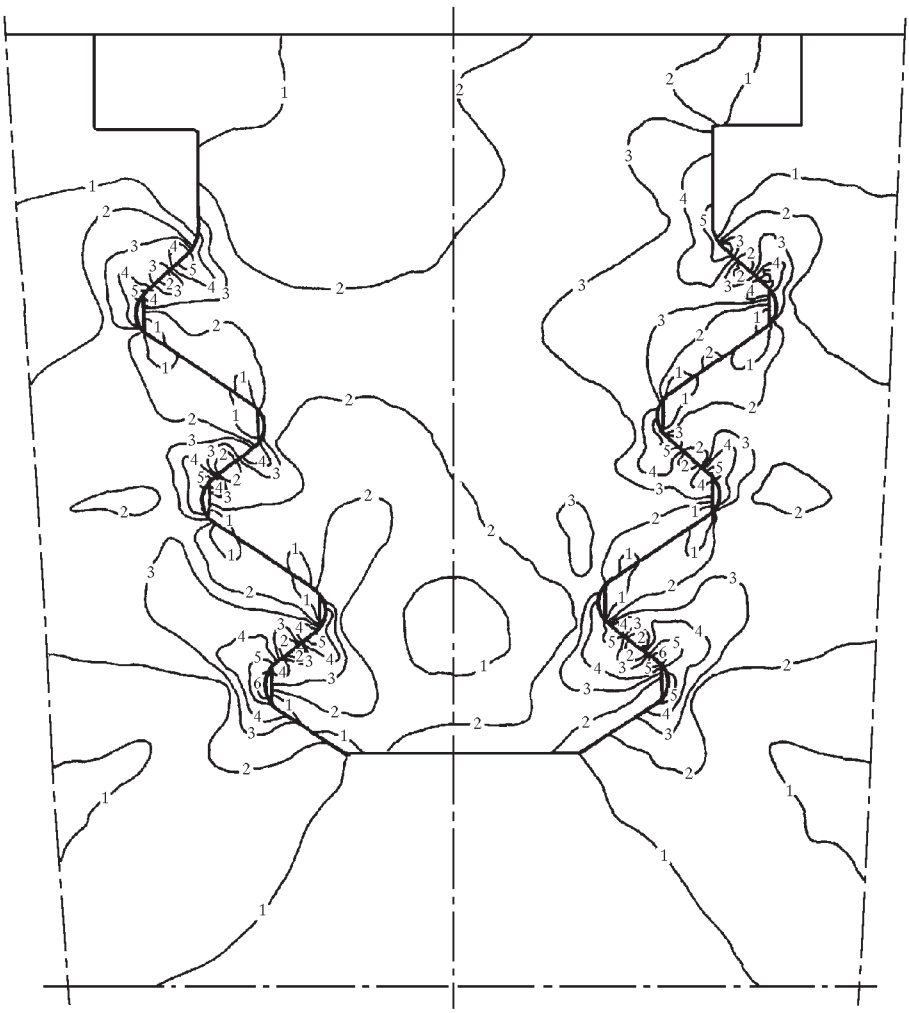

Fig. 5. Elasto-plastic effective stress in the cross-section of the attachment

faces as a function of friction coefficient are presented (see Table 3 below). For cases 1 and 4 also the initial and resultant contact statuses of contact nodes within maximally stressed contact surfaces are shown in Table 4.

Table 3. Maximal normal contact stresses for the elasto-plastic cases 1-4

Case	Normal contact stresses $[10^8\,\mathrm{N/m^2}]$					
	Location (lowest right hooks)			Location (highest left hooks)		
	Right edge	Middle	Left edge	Right edge	Middle	Left edge
1	4.384	1.562	2.832	2.891	1.826	2.833
2	3.989	1.250	2.889	2.602	1.589	2.861
3	3.858	1.172	3.002	2.457	1.479	2.918
4	3.814	1.125	3.036	2.371	1.443	2.946

Table 4. Map of initial and resultant contact status for elasto-plastic cases 1 and 4

Case	Node location	Initial and resultant status of contact nodes											
		Node layer (lowest right hooks)						Node layer (highest left hooks)					
		1	2	3	4-10	11	12	1	2	3	4-10	11	12
1	Right	S	S	S	S	S	S	S/G	S	S	S	S	S/G
	Middle	S	S	S	S	S	S	S	S	S	S	S	S
	Left	S	S	S	S	S	S	S	S	S	S	S	S
4	Right	A/S	A/S	A/S	A/S	A/S	A/S	A/G	A/S	A/S	A/S	A/S	A/G
	Middle	A/S	A/S	A/S	A/S	A/S	A/S	A/S	A/S	A/S	A/S	A/S	A/S
	Left	A/S	A/S	A/S	A/S	A/S	A/S	A/S	A/S	A/S	A/S	A/S	A/S

The stress distribution within the attachment is typical, that is high values of effective stresses appear at the minimum neck sections or the adjacent contact surfaces of the root and disc, and the maximal values correspond to the first root and third disc hooks. Note, however, that the elasto-plastic deformations occur only for the latter hooks. It is interesting to notice again that inclusion of friction ($\mu = 0$ in comparison to $\mu = 0.05$) changes the values of contact stresses much more than further increase of the friction coefficient ($\mu = 0.10$ and $\mu = 0.15$). Again, inclusion of friction diminishes the contact stresses and does not affect the tendency to gap appearance.

Comparing the results of the values of the normal contact stresses from Tables 1 and 3 one can notice that inclusion of friction changes these values more significantly in the elastic case. Also, a tendency to gap appearance is stronger for that case (compare Tables 2 and 4). These two observations can be atributted to smaller effective stresses within the attachment operating in the elastic range.

4. Conclusions

It is possible to generate one general FE algorithm conforming both to the Coulombian and elasto-Coulombian slip rules for incremental contact problems of elasticity and elasto-plasticity as applied to three-dimensional turbomachinery blade attachment analysis.

Physical non-linearity of contact problems due to friction plays an important role in the stress analysis both in the elastic and elasto-plastic range. In the case of the attachments under consideration, inclusion of friction changes the effective stresses at the hook notches and a tendency to reduce them prevails. Also a tendency to change the distribution and to reduce the normal contact stresses appears.

On the contrary, inclusion of friction does not seem to affect the gap appearance within contact surfaces for both the cases of elastic and elasto-plastic analysis.

In the case of highly stressed attachments (which may include also elasto-plastic deformation), changes of the normal contact stresses due to inclusion of friction are weaker than in the case of less-stressed attachments. A tendency to gap appearance is weaker for highly stressed attachments.

References

1. Alderson R.G., Tani M.A., Tree D.J., 1967, Three-Dimensional Optimization of a Gas Turbine Disk and Blade Attachment, *J. Aircraft*, **13**, 994-998

2. Bloch M.V., Orobinskiĭ A.V., 1983, O Modifikacii Metoda Konechnykh Elementov dlja Resheniya Dvumernykh Uprugikh i Plasticheskikh Kontaktnykh Zadach, *Problemy Prochnosti*, **5**, 21-27

3. Chan S.K., Tuba I.S., 1971, A Finite Element Method for Contact Problems of Solid Bodies. Part II – Application to Turbine Blade Fastenings, *Int. J. Mech. Sciences*, **13**, 627-639

4. Gontarovskiĭ P.P., Kirkač B.N., 1982, Issledovanie Napryazhenno-Deformirovannogo Sostoyaniya Zamkovykh Soedineniĭ Lopatok Turbomashin Metodom Konechnykh Elementov, *Problemy Prochnosti*, **8**, 37-40

5. Gontarovskiĭ P.P., Kirkač B.N., Marcenko G.A., 1978, Priblizhennyĭ Metod Rascheta Zamkovykh Soedineniĭ Lopatok Turbomashin, *Problemy Mashinostroeniya*, **6**, 52-55

6. IKEDA T., HISA S., MATSUURA T., 1989, The Development of a Titanium Last-Stage Blade for 3600 rpm Steam Turbines, *Latest Advances in Steam Turbine Design, Blading, Repairs, Condition Assessment, and Condenser Interaction*, PWR-7, 69-76, ASME, New York

7. MEGUID S.A., KANATH P.S., CZEKANSKI A., 2000, Finite Element Analysis of Fir-Tree Region in Turbine Discs, *Finite Elements in Analysis and Design*, **35**, 305-317

8. NIGIN A.A., 1976, Rashchët Elochnogo Zamka, *Izv. Vysshykh Uceb. Zavedenič. Mashinostroenie*, **2**, 17-21

9. RAO J.S., RAMAKRISHNAN C.V., GUPTA K., SINGH A.K., 2000, Elasto-Plastic Stress Analysis of LP Steam Turbine Blades under Centrifugal Loading, *J. Turbomachinery* (to appear)

10. ROBERTSON M.D., WALTON D., 1990, Design Analysis of Steam Turbine Blade Roots under Centrifugal Loading, *Journal of Strain Analysis for Engineering Design*, **25**, 185-195

11. TEPER B., MOORE C.T., 1989, The Redesign of a Fir Tree Blade Root for the Penultimate Stage of a 500 MW Turbine, *Latest Advances in Steam Turbine Design, Blading, Repairs, Condition Assesment, and Condenser Interaction*, PWR-7, 17-22, ASME, New York

12. ZBOIŃSKI G., 1992, Numerical Contact Analysis of Turbomachinery Blade Attachments, *Archives of Mechanical Engineering*, **32**, 317-331

13. ZBOIŃSKI G., 1993a, FE Algorithm for Incremental Analysis of Large 3D Frictional Contact Problems of Linear Elasticity, *Computers and Structures*, **46**, 669-677

14. ZBOIŃSKI G., 1993b, FE Computer Program for Incremental Analysis of Large 3D Frictional Contact Problems of Linear Elasticity, *Computers and Structures*, **46**, 679-687

15. ZBOIŃSKI G., 1993c, Incremental Variational Principles for Frictional Contact Problems of Linear Elasticity, *ASME J. Appl. Mech.*, **60**, 982-985

16. ZBOIŃSKI G., 1993d, Numerical Research on 3D Contact Problems of Turbomachinery Blade Attachments in the Elastic Range, *Int. Journal of Mechanical Sciences*, **35** (1993), 141-165

17. ZBOIŃSKI G., 1993e, The Incremental Variational Principle and Finite Element Displacement Approximation for Frictional Contact Problem of Linear Elasticity, *Journal of Non-Linear Mechanics*, **28**, 13-28

18. ZBOIŃSKI G., 1995a, Derivation of the Variational Inequalities of the Incremental Frictional Elastic Contact Problems, *Archives of Mechanics*, **47**, 725-743

19. Zboiński G., 1995b, Physical and Geometrical Non-Linearities in Contact Problems of Elastic Turbine Blade Attachments, *Proc. of the Instn. of Mechanical Engineers. Part C: Journal of Mechanical Engineering Sciences*, **209**, 273-286

20. Zboiński G., Ostachowicz W., 1997a, A General FE Algorithm for 3D Incremental Analysis of Frictional Contact Problems of Elasto-Plasticity, *Finite Elements in Analysis and Design*, **27**, 289-305

21. Zboiński G., Ostachowicz W., 1997b, A General FE Computer Program for 3D Incremental Analysis of Frictional Contact Problems of Elasto-Plasticity, *Finite Elements in Analysis and Design*, **27**, 307-322

22. 1995, *ABAQUS. Theory Manual, Version 5.5*, Hibbit, Karlsson and Sorensen, Inc., Pawtucket, RI (USA)

23. 1995, *MSC/NASTRAN. Release Notes for Version 68*, The MacNeal-Schwendler Corporation, Los Angeles, CA (USA)

24. 1999, *Automatic Dynamic Incremental Nonlinear Analysis. Theory and Modeling Guide. Volume I: ADINA*, Report ARD 99-7, ADINA R & D, Inc., Watertown, MA (USA)

Trójwymiarowa analiza kontaktowa z tarciem zamocowań łopatek maszyn wirnikowych w zakresie sprężystym i sprężysto-plastycznym

Streszczenie

Niniejsza praca przedstawia podsumowanie wyników badań nad trójwymiarową analizą kontaktu w zamocowaniach łopatek maszyn wirnikowych w zakresie sprężystym i sprężystoplastycznym. W tym kontekście zaprezentowane zostały istotne aspekty analizy związane z teoretycznym, metodologicznym i fenomenologicznym opisem problemu. Praca koncentruje się na zastosowanych sformułowaniach wariacyjnych problemów kontaktowych sprężystości i sprężysto-plastyczności, odpowiadających im metodach elementów skończonych, zaproponowanych algorytmach kontaktowych, a także opisach stanów przemieszczeń, naprężeń, kontaktu i poślizgów w rzeczywistych zamocowaniach łopatek turbinowych. Ze szczególną uwagą potraktowano problemy nieliniowego charakteru algorytmów kontaktowych oraz wpływu tych nieliniowości na naprężenia i odkształcenia w zamocowaniu.

Manuscript received December 11, 2000; accepted for print February 20, 2001